Network of European Research Infrastructures for Earthquake Risk Assessment and Mitigation

Report

Implementation report

Activity:	*Near fault ground motion*
Activity number:	*JRA3, Task 13.7*
Deliverable:	*Report and electronic database*
Deliverable number:	*D13.5*
Responsible activity leader:	*Luis Dalguer(ETH, now at swissnuclear)*
Responsible participant:	*ETHZ*
Author:	*Luis Dalguer(ETH, now at swissnuclear)* Aysegul Askan *(METU) and Seok Goo Song (ETH, now KIGAM)*

Seventh Framework Programme
EC project number: 262330

Structure of the deliverable

1. Summary of the Significance of the Project

This JRA3 work package (WP13) developed and applied state-of-the-art physics-based numerical techniques for earthquake rupture modeling to quantify statistical properties of ground-motion variability dominated by the source for engineering needs. We have brought together competences in physics based numerical modeling of waveform propagation and frictional sliding to simulate the complexity of earthquake source (kinematically and dynamically) and near-source broadband ground motion (deterministic and stochastic), with the final goal to quantify statistical properties of ground-motion variability and to propose physics-based Ground Motion Prediction Equations (GMPE) for engineering needs. This ultimate goal (the new GMPE) was not fully accomplished, it is an ongoing work. Nevertheless we present a preliminary GMPE (as milestone) developed to date. In addition, here we summarize the available data and the tools and software developed during the project to reach our goal. The data comprise a database of 360 synthetic physics-based earthquakes used to investigate the feasibility of the development of physics-based GMPEs and to study the effects of source parameters on ground motion predictions and the sensitivity of near-source ground motion to source (correlation) statistics. The tools and software comprise earthquake rupture and ground motion generators used to study source complexity and the near-field ground motion spatial variability.

2. Results

We have developed research on earthquake source and near-field ground motion in different fronts using physics-based numerical model. In APPENDIX is a summary of such contributions per institute. A full description in detail of such research developed per institute can be found in deliverable 13.4 (D13.4). Though the results in D13.4 were not fully quantitatively integrated to reach our ultimate goal, that is the implementation of new GMPE, there is a qualitative input that has guided us to incorporate (or plan to incorporate) elements or terms into the new GMPE to account for source effects not traditionally considered in published GMPEs.

The implementation of a new GMPE in this work package is a direct joint effort between ETH and METU. First we report the implementation of a preliminary GMPE with simplified functional form. Second we report an ongoing work of GMPE that incorporate source complexity effects (from hanging wall and directivity) and oversaturation of ground motion very near the source. This latter implementation is expected to have a final GMPE by the end of 2015.

2.1 Implementation of a simplified physics-based GMPE

We summarize here the key results obtained by parameterising a near-field synthetic waveform dataset based of 360 dynamic rupture models (Baumann and Dalguer, 2014) in the moment magnitude range $5 < M_W < 7+$ relevant for seismic hazard studies in central and Western Europe. Baumann and Dalguer (2014) showed that peak ground-motion values obtained through dynamic-rupture numerical simulations of strong ground-motions are compatible – at least in statistical sense – with state-of-the-art empirical prediction tools in a frequency range up to 1.0Hz. So the derived GMPE is considered valid withink this frequency range. The 360 rupture models consider 3 style of faulting (SOF): strike-slip, normal and reverse; one single soil profile, representative of hard-rock condition (Vs30 ≈2500 m/s); 2 fault cases: buried faults and surface-rupturing faults; 2 extreme cases of normal stress: depth-dependent and depth-independent. There are 30 model for each case (30 x 3 SOF x 4= 360). In the set of 30 models the Mw varies according to the dynamic rupture model (see Figure 1).

A subset of the provided ground motions has been selected. Although the sites distribution adopted for the calculations allows to have source-to-site distances up to 70-80 km, we restricted the data to Rjb distances < 30 km. This is done for two reasons: 1. We are interested in the near-fault GM and 2. this reduces the effect of attenuation (and thus regional character) of the GM simulation model. The Pseudo Spectral Acceleration (PSA) 5% damped is used. The frequency limit imposed by the maximum resolvable frequency in the calculations is 3 Hz. Thus we calculate PSA for periods >= 0.4s. The geometric mean of horizontal components is used in the regression analyses.

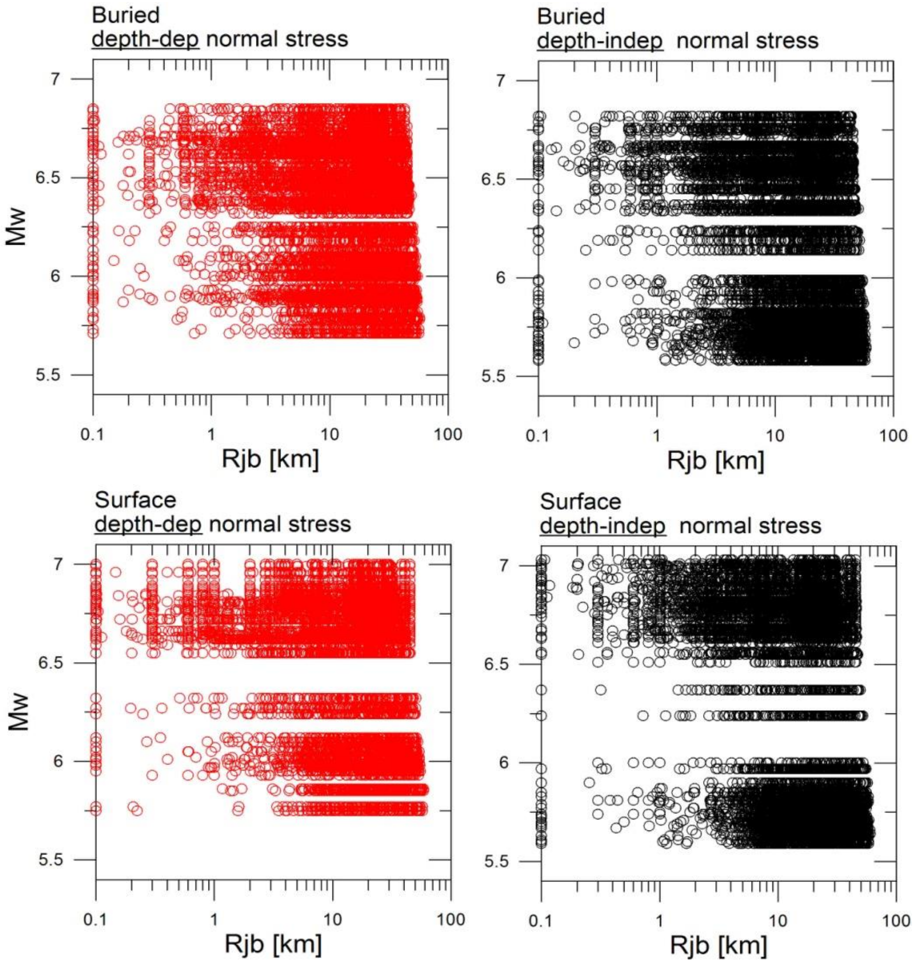

Figure 1. Magnitude-distance distribution of the 4 Datasets used in the study.

The functional form adopted is a simplified version of that typically adopted in recent empirical GMPEs (Boore and Atkinson, 2008; Akkar and Bommer, 2010). With respect to current empirical GMPEs a number of simplifications are introduced in the functional form, due to the particular dataset used in this study. In particular:
-no site coefficient is used, because all the site have the same site conditions;
- no M-dependent distance decay is used, as the distance and M ranges are quite small
- no anelastic attenuation term is used (linear decay in the log space)
- no saturation with M (M-squared term) is used, because the M-scaling of PSA does not show apparent magnitude saturation (at least up to Mw=7).

The functional form finally retained is:

$$\log_{10}(Y) = a + F_D(R) + F_M(M) + F_{SOF}$$

$$F_D(R) = c_1 \log 10\left(\sqrt{R_{JB}^2 + h^2}\right)$$

$$F_M(M) = \begin{cases} b_1(M - M_h) & \text{for } \mathrm{M} \le \mathrm{M_h} \\ b_2(M - M_h) & \text{otherwise} \end{cases}$$

where a, c1, b1 and b2 are coefficients to be determined in the regression. F_{SOF} represents the style of faulting correction and it is given by $F_{sof} = f_j E_j$, for j=1,…,3, where f_j are the coefficients to be determined during the analysis and E_j are dummy variables used to denote the different fault classes. We considered 3 types of style of faulting: reverse (R), strike slip (SS), normal (N) and constrained f_3=0 (Normal faults) at all periods. The regressions are performed using a maximum likelihood approach and the random effects model is used to separate the within-event and between-event variabilities (e.g. Brillinger & Preisler, 1985; Abrahmson and Youngs, 1992). The coefficients for the 4 models are presented in Table 1.

Preliminary Observations (see Figures 2-4):

- The residuals do not show any clear dependencies on M and R suggesting that the functional form is adequate in explaining the average characteristics of GM.
- Difference between the models is larger for small magnitudes.
- Usually depth-dependent normal stress (DD) is larger than depth-independent normal stress (NND).
- Surface faulting is larger than Buried up to about 10 km, then very close.
- Distance decay is different. h coefficients (controlling the plateau) is larger for buried faults. surface faults GM starts to decay at shorter distances.
- A clear correlation is found between with Vr (at both periods) and maximum stress drop (mostly at short periods). On the other hand, no apparent correlation is found with average stress drop. This results mean that all the events that have e.g., a Vr larger than 2.3 km/s produce GM that are on average larger than the mean prediction. Including the Vr in the functional form will remove this trend in the residuals.
- The residuals for strike-parallel stations show a larger residual dispersion with respect to the other stations. This indicates that some effects that depend on the source-site geometry (e.g., directivity) is not captured by the preliminary model).

Table 1. Model coefficients

Surface rupturing fault , depth independent normal stress (SURF-NDD)										
T	a	b1	b3	c1	h	f1	f2	sigmabetween	sigmawithin	sigmaTOT
0.4	2.14416	0.08204	1.23297	-0.72888	2.72605	0.115197	0.053022	0.0921	0.2930	0.3071
0.5	2.17127	0.103157	1.26133	-0.6815	2.68914	0.099386	0.045775	0.0925	0.2940	0.3082
0.6	2.18763	0.125978	1.23899	-0.66294	2.76945	0.090833	0.048198	0.0916	0.2912	0.3052
1	2.10748	0.136442	1.07357	-0.6337	2.88742	0.101334	0.039525	0.0913	0.2740	0.2888
2	1.80097	0.159851	0.990765	-0.62201	3.15688	0.129248	0.02424	0.0934	0.2528	0.2695
3	1.65968	0.356626	1.01802	-0.65032	4.00697	0.122615	0.028539	0.0905	0.2575	0.2729
4	1.62773	0.473296	1.10117	-0.75176	5.65843	0.130868	0.039752	0.0845	0.2534	0.2671
5	1.4526	0.559903	1.14268	-0.6974	5.98559	0.143768	0.041952	0.0828	0.2483	0.2617
Surface rupturing fault , depth dependent normal stress (SURF-DD)										
T	a	b1	b3	c1	h	f1	f2	sigmabetween	sigmawithin	sigmaTOT
0.4	1.98101	-0.29564	1.27092	-0.59556	2.52308	0.089244	0.064978	0.0937	0.2664	0.2824
0.5	2.01817	-0.25838	1.24605	-0.55179	2.42129	0.077522	0.072657	0.0943	0.2681	0.2842
0.6	2.02695	-0.2396	1.20935	-0.52653	2.30968	0.069035	0.08702	0.0885	0.2656	0.2800
1	2.01963	-0.2439	1.12096	-0.55104	2.7889	0.069213	0.087391	0.0876	0.2491	0.2640
2	1.76813	-0.21697	1.15904	-0.61735	2.90216	0.061529	0.0595	0.0886	0.2292	0.2457
3	1.54149	-0.06735	1.21135	-0.6347	2.96519	0.091964	0.061244	0.0823	0.2470	0.2603
4	1.42947	0.042432	1.26877	-0.6949	3.60371	0.123824	0.058668	0.0739	0.2507	0.2613
5	1.20312	0.14512	1.32626	-0.59891	3.20856	0.154071	0.039256	0.0742	0.2516	0.2623
Buried fault , depth independent normal stress (BUR-NDD)										
T	a	b1	b3	c1	h	f1	f2	sigmabetween	sigmawithin	sigmaTOT
0.4	1.94712	0.158985	1.04072	-0.53111	4.25783	0.045921	0.050829	0.0965	0.2613	0.2786

0.5	2.03122	0.178348	1.02603	-0.52459	4.84369	0.032658	0.045476	0.0975	0.2640	0.2815
0.6	2.06395	0.194139	0.992202	-0.51674	5.14724	0.023256	0.04337	0.0978	0.2647	0.2822
1	1.94372	0.180072	0.918981	-0.48334	4.94418	0.035985	0.056486	0.1012	0.2507	0.2704
2	1.626	0.157693	0.92506	-0.50661	4.07988	0.042965	0.066189	0.0977	0.2237	0.2441
3	1.50531	0.314199	0.89673	-0.58989	4.35943	0.05412	0.056287	0.1014	0.2240	0.2458
4	1.53282	0.455016	0.906286	-0.71756	6.5574	0.075667	0.041666	0.1024	0.2263	0.2484
5	1.38612	0.576518	0.8959	-0.65722	7.38325	0.092422	0.033071	0.1034	0.2284	0.2507
Buried fault , depth dependent normal stress (BUR-DD)										
T	a	b1	b3	c1	h	f1	f2	sigmabetween	sigmawithin	sigmaTOT
0.4	2.035	0.010558	0.85159	-0.52072	5.00664	0.02769	0.013328	0.1017	0.2504	0.2702
0.5	2.06633	0.028082	0.832959	-0.48068	4.87442	0.0243	0.014217	0.1025	0.2518	0.2719
0.6	2.10513	0.031403	0.852477	-0.48261	5.07675	0.015832	0.008334	0.1040	0.2537	0.2742
1	2.01905	-0.0018	0.819481	-0.46393	4.70481	0.019823	0.012114	0.1029	0.2399	0.2611
2	1.78149	0.03802	0.878131	-0.54008	4.56687	0.013191	0.008498	0.1107	0.2113	0.2385
3	1.59532	0.190351	0.90645	-0.59345	4.29455	0.022351	-0.00769	0.1091	0.2135	0.2398
4	1.62167	0.316547	0.950777	-0.7452	6.09221	0.036933	-0.01934	0.1028	0.2178	0.2408
5	1.41596	0.429654	0.997622	-0.65704	6.27676	0.055133	-0.03539	0.1038	0.2245	0.2474

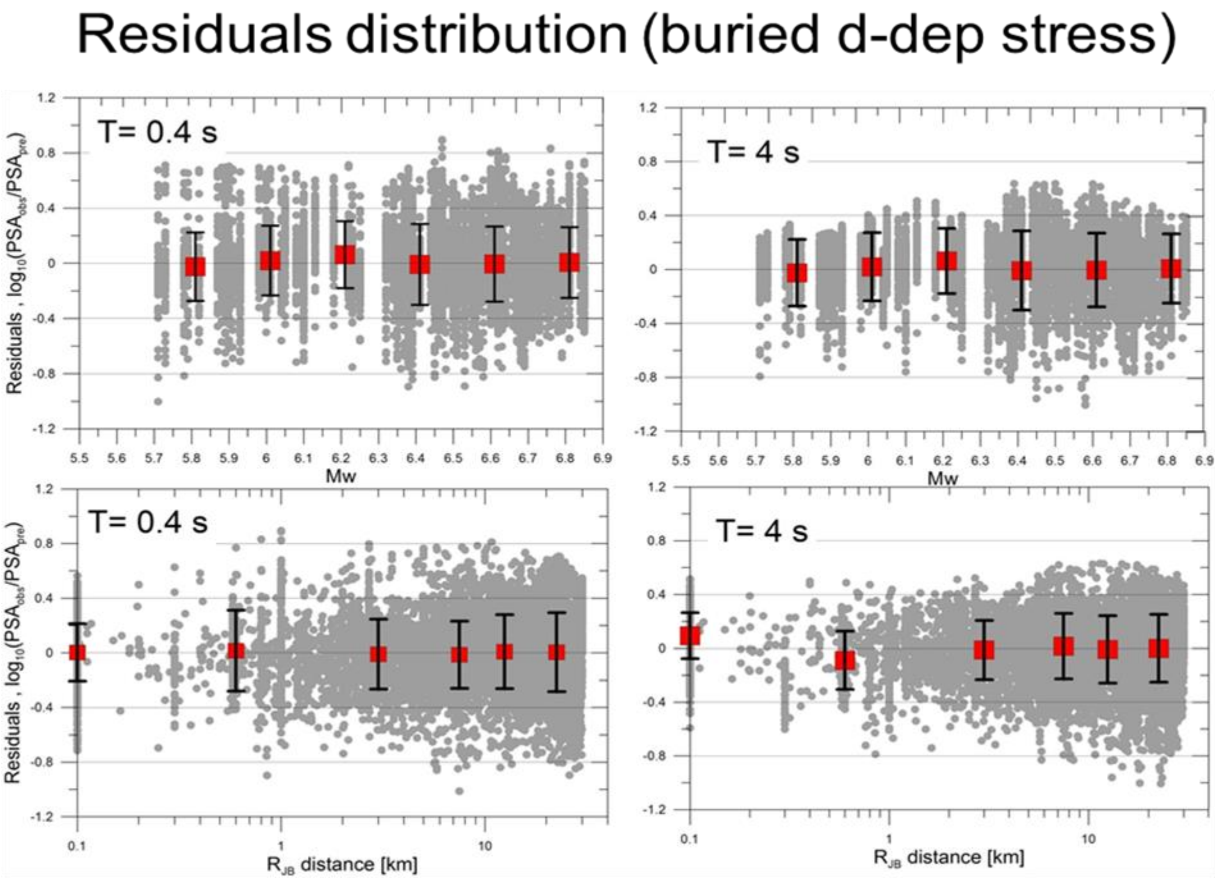

Figure 2. Residual (log10(PSAobs/PSApre)) as a function of magnitude and distance for the buried depth-dependent stress model at two spectral periods. Mean and standard deviation of residuals over M and R bins are also showed.

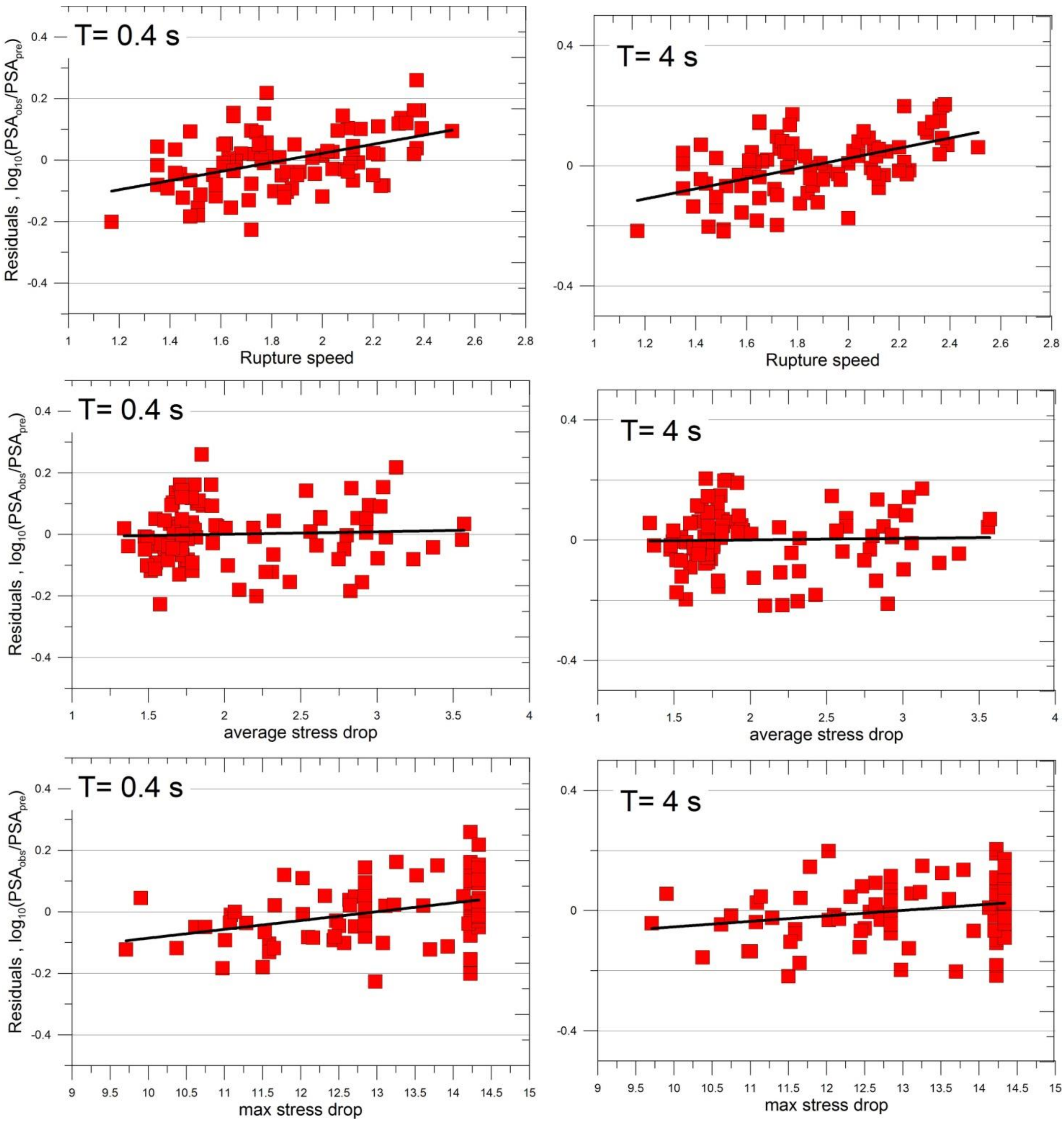

Figure 3. Between-event residuals for the BUR DD model plotted as a function of rupture speed, average stress drop (Mpa) and maximum stress drop (Mpa) for 2 spectral periods. The LSQR linear fit in also showed as a black line.

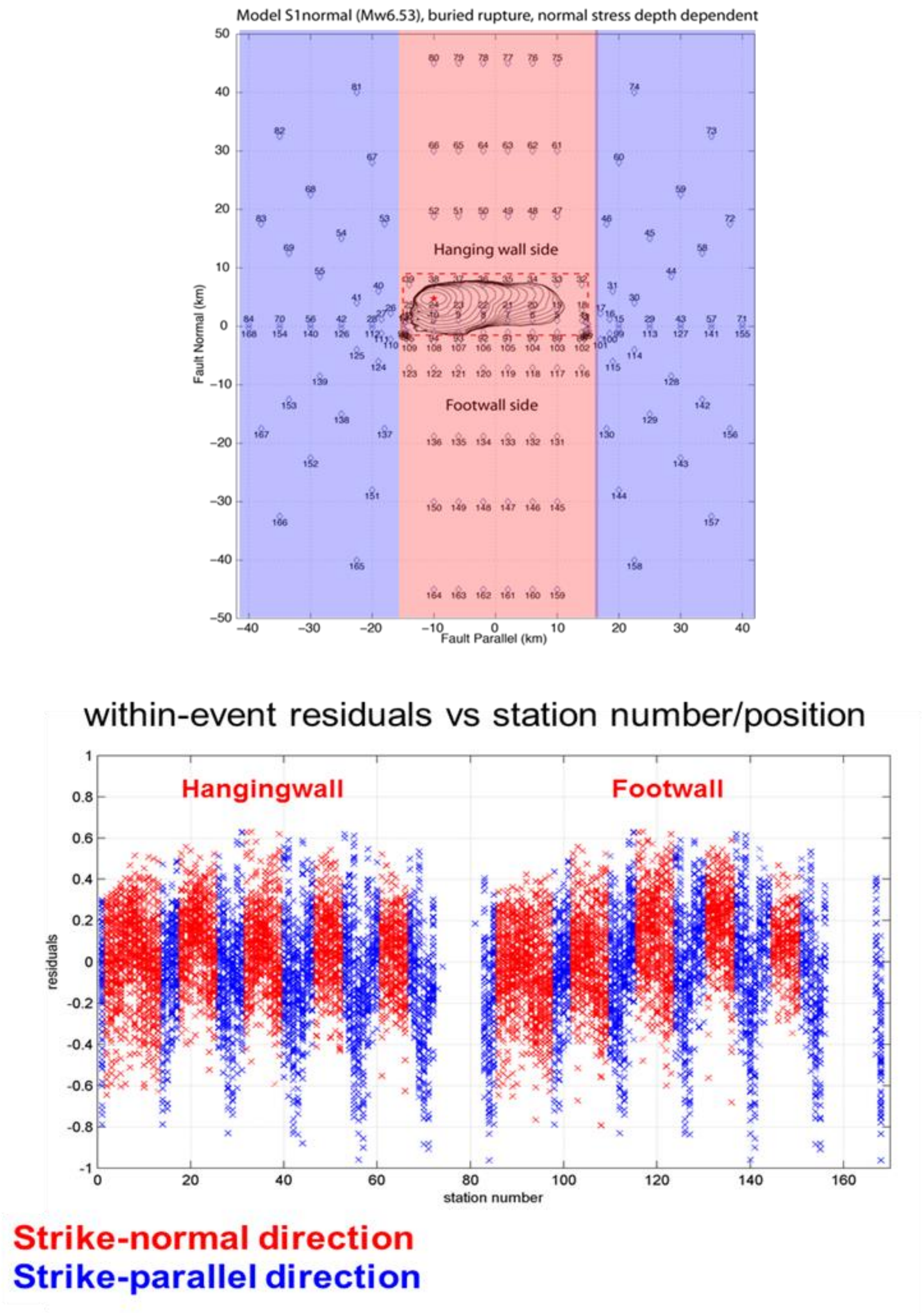

Figure 4. Within-event residuals versus station number and position. In Blue are marked stations in the fault strike direction and in red stations in the fault parallel direction.

2.2 Ongoing work on the implementation of physics-based GMPE

Source effects from hanging wall and directivity, as well as oversaturation of ground motion near the source observed in the 360 dynamic rupture models are parameterized here. The work is an ongoing effort in collaboration with Carlo Cauzzi from ETH. The main findings of this effort are reported here:

The residual between the 360 dynamic rupture models and current empirical GMPEs (Akkar et al., 2014) are computed (Fig. 5). Trends are apparent in the data distribution as a function of magnitude and distance. That is, the functional forms typically adopted for empirical predictions of peak ground-motions and response spectra cannot be directly used to fit synthetic near-field ground-motion data or, in other words, the particular features of near-field ground-motions are not captured by the relatively simple parameterisation of current empirical GMPEs.

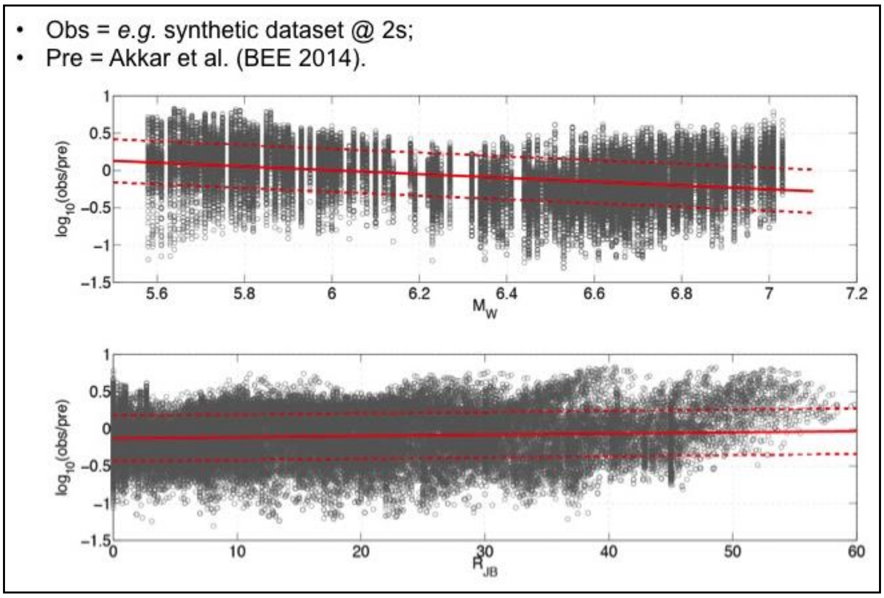

Figure 5 – Residuals of the 360 synthetic dataset with respect to the empirical prediction model of Akkar et al. (2014).

We used the 360 rupture models - see also Cauzzi and Dalguer (2012) and Baumann and Dalguer (2013) - to investigate the variation of near-field peak ground-motion and response spectra with

- Moment magnitude M_W;
- finite-fault distance (both R_{RUP} and R_{JB});
- near-source characteristics like the hanging-wall / foot-wall location, directivity and radiation pattern effects.

We used synthetics: a) to overcome the difficulties posed by the paucity of near-field data in the calibration datasets of empirical ground-motion prediction equations (GMPEs); b) to expand our understanding of source-dominated ground-motion phenomena; c) to investigate the characteristics of "noise-free" long-period ground motions. The most interesting (*i.e.* different from the current GMPE approaches) results that we obtained are selectively summarized in the following paragraphs.

Linear scaling with magnitude for vibration periods larger than 2 s, where the numerical simulations contain enough energy to be considered technically reliable (Fig. 6). The prediction of magnitude scaling would then use one predictor (M_W) and two period-dependent coefficients. This is consistent with the functional form adopted by Cauzzi and Faccioli (2008), who used a worldwide databank – albeit dominated by Japanese data – to derive long-period spectral predictions for M_W 5-7+. Note that the same authors (Cauzzi et al., 2014) used recently a quadratic scaling with magnitude – as many other GMPE modelers do – as a result of enlarging their original dataset to the range 4-8.

Amplification factors due to style-of-faulting. We found that the faulting style can be reasonably modeled by means of amplifications factors for normal and reverse and strike-slip mechanism with respect to unspecified (Fig. 6). That is, using dummy variables for different faulting styles when performing regressions on the synthetic dataset. The prediction of style-of-faulting impact would then use three predictors (*N*, *R*, *S*) and three period-dependent coefficients.

Attenuation with finite-fault distance metrics R_{JB} and R_{RUP}. We found that classical functional forms based on the geometric attenuation of spectral amplitude with distance are valid for the synthetic dataset but (Fig. 7):

- a magnitude dependent geometric decay could be explicitly modeled only if R_{RUP} was used as predictor;
- a magnitude-dependent saturation with distance could be explicitly modeled only if R_{RUP} was used as predictor;

- the fictitious depth h to be used with R_{JB} could be modeled as a function of the depth to the top of rupture Z_{TOR};
- data showed larger dispersion if represented as a function of R_{JB}.

Therefore modeling the attenuation with distance required using two predictors and up to four period-dependent coefficients.

Near-source oversaturation of spectral amplitudes generated by strike-slip events. Similar to Graizer et al. (2013) we observed oversaturation of spectral values for distances shorter than the depth to the top of rupture (Z_{TOR}) and we attributed this observation to a radiation pattern effect (Fig. 4). This near-source oversaturation effect can be reasonably modeled as a cosine taper for distances shorter than (Z_{TOR}) as shown in Fig. 8, *i.e.* using two predictors and two period-dependent coefficients. Note that strike-slip events in the dataset occur on vertical faults only.

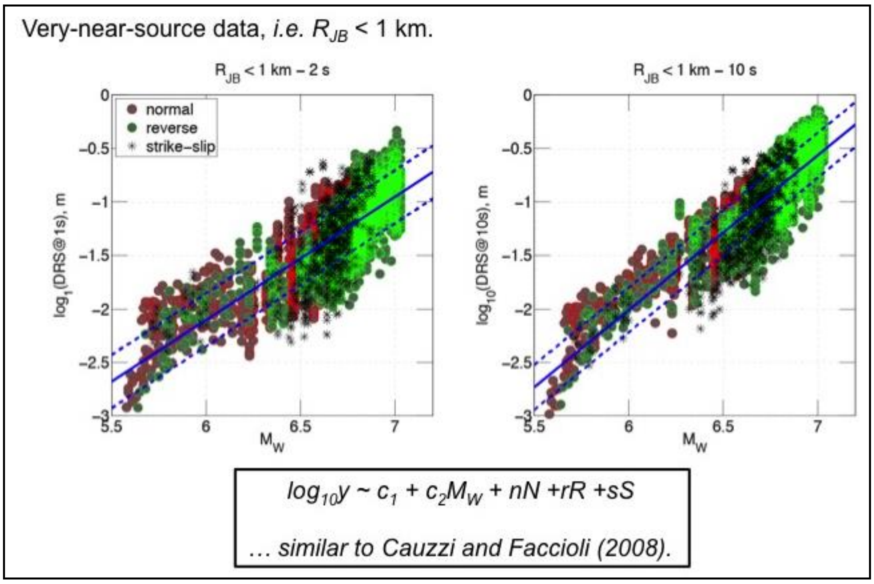

Figure 6 – Magnitude scaling and style-of-faulting effect at a glance.

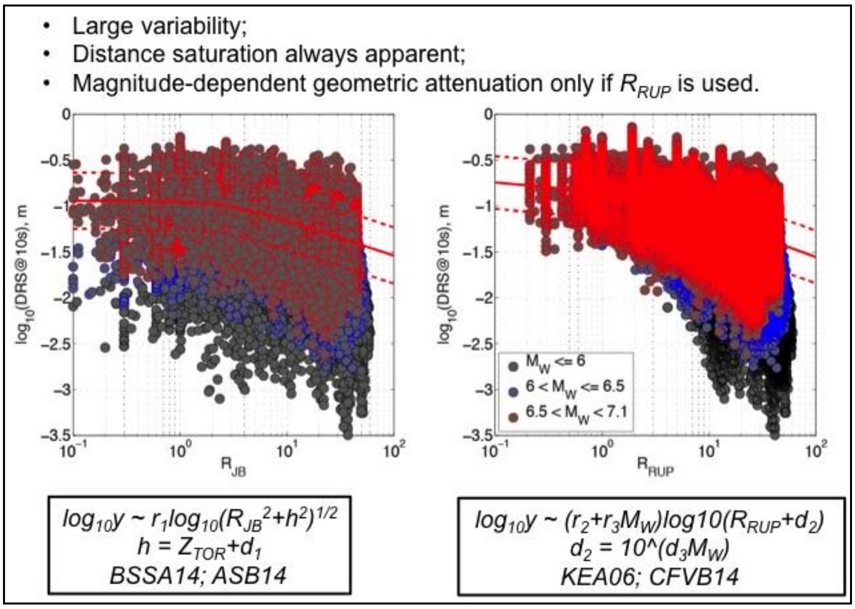

Figure 7 – Geometric attenuation of long-period spectral ordinates with finite finite fault distance metrics R_{JB} and R_{RUP}.

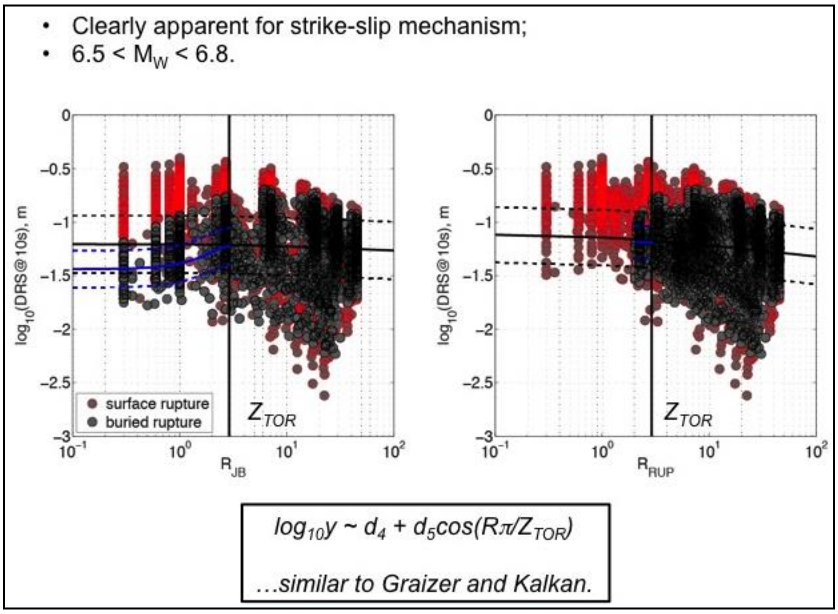

Figure 8 – Near-source oversaturation of spectral amplitudes generate by strike-slip vertical fault events.

Hanging-wall amplification effect. Consistent with the latest approaches developed within the NGA project, we found a clear signature of increased spectral levels at stations located on the hanging-wall side of large-magnitude dipping-fault events. Our results show that the hanging-wall effect is a quadratic function of the distance from the fault strike (R_X) within the surface projection of the ruptured fault, and a cubic decreasing function of R_X otherwise. That is, the hanging-wall term parameterisation requires one predictor (R_X) and up to three period-dependent coefficients (Fig. 9).

Directivity. We could explain the lower and upper bounds of the synthetic spectral amplitudes based on directivity. We found that the approach developed by Bayless and Somerville within NGA West-2 (see Spudich et al., 2014) seems to apply also for the 360 synthetic dataset, as shown in Fig. 10.

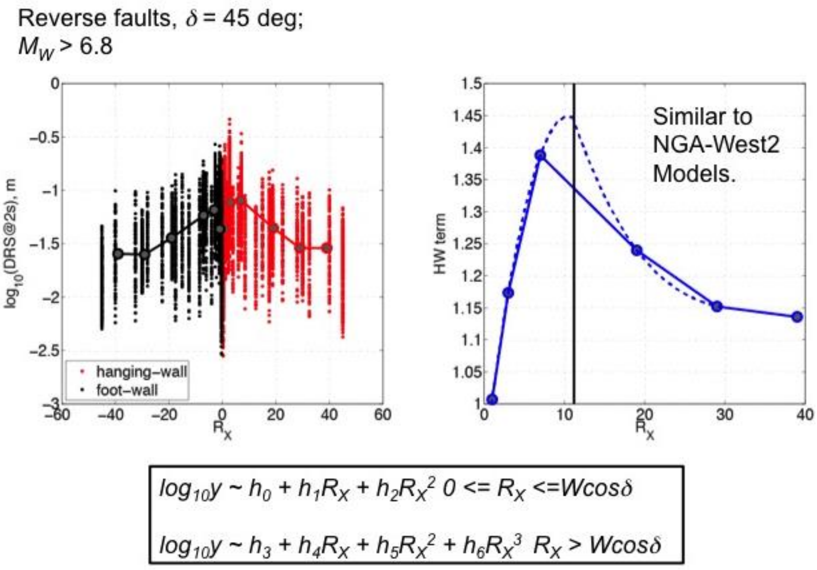

Figure 9 – Near-source oversaturation of spectral amplitudes generate by strike-slip vertical fault events.

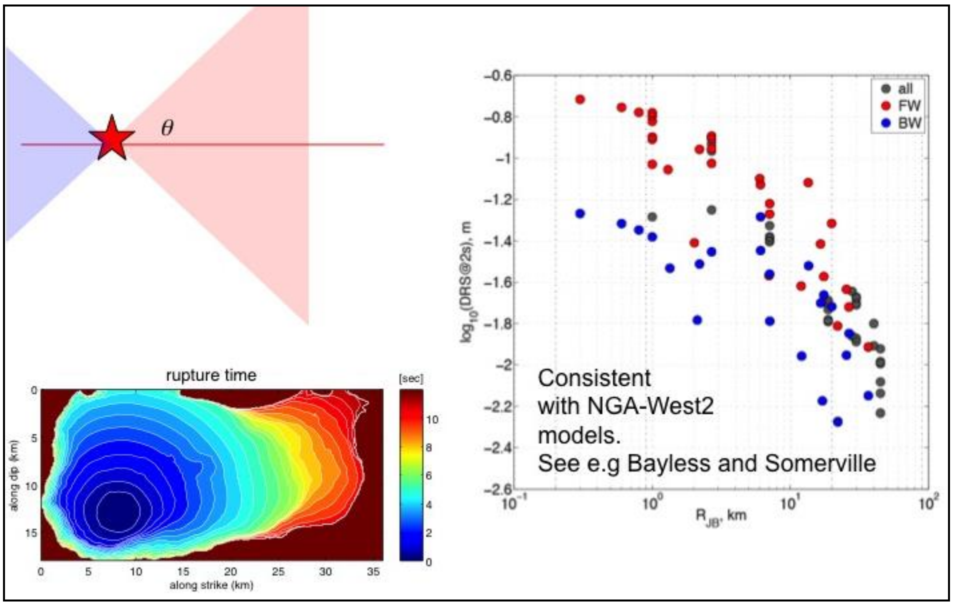

Figure 10 – Effect of directivity on the simulated spectral amplitudes.

3. Implementation and Dissemination

The database used for the implementation of the GMPEs, main software and tools developed in this work package have been reported in deliverable 13.3, in which include detail description of the methodology, applications, examples, related publications and availability. Here we make a short description of these implementations and how they can be accessible, this list includes the GMPEs described above.

- **Simplified GMPE.** This model predictor is fully described above. This product has not been published yet, but for more details of the functional form parameterization can be obtained by direct contact to Aysegul Askan from METU (aaskan@metu.edu.tr).

- **GMPE that incorporates source effect complexities.** As described above, the implementation of this model predictor is currently in progress. More detail description can be obtained by direct contact to Carlo Cauzzi from ETH (carlo.cauzzi@sed.ethz.ch) or Luis Dalguer from swissnuclear (luis.dalguer@swissnuclear.ch). Preliminary results of this model have been presented in conferences (Dalguer et al, 2013, 2014 and Cauzzi et al, 2014b).

- **EGF_K2 ground motion generator**. This code combines the complexity in source kinematics with empirical Green functions. This method can be used to simulate synthetic seismograms up to 20 Hz. It has been developed in **AMRA, ISTerre.** The software is available on demand to Sergio Del Gaudio (sergio.delgaudio@unina.it).

- **KIRIA.** It is a source inversion software that generates kinematic source models using strong-motion, GPS and SAR data. It is based on a global exploration and 1D numerical Green's function. It has been developed in **INGV, USGS.** The software is available on demand (antonella.cirella@ingv.it, alessio.piatanesi@ingv.it); to date there is not t a user manual for this software.

- **Pseudo-dynamic Rupture Model Generator,** SongRMG, version 1. It is a code used to extract one-point and two points statistics from an ensemble of source models. The main functionality of this code is to provide kinematic models whose characteristics are compatible with rupture dynamics. They can be used as input source models for ground motion generation or to constrain inverse problems. The code has been developed in ETH and is available on demand to Dr. S.G. Song (sgsong@kigam.re.kr). It will be available to the public soon.

- **Database of synthetic earthquakes.** Data consist of final slip, peak slip rate, rupture time of 360 dynamic rupture models in the range of Mw ~5.5-7.0 and resulted near-field synthetic seismograms on a dense near-source receiver grid. The models are for three classes of faulting (thrust, normal and strike slip) for buried and surface-rupturing earthquakes. Stress and frictional strength consider two extreme cases of normal stress, 1) depth-dependent, and 2) depth-independent. The database of the 360 dynamic rupture models is available to download from http://www.seg2.ethz.ch/dalguer/download/DynaModels360.html or asking directly to Dr.Luis A. Dalguer (luis.dalguer@swissnuclear.ch).

4. Conclusion

We have compiled a list of main outputs (ground motion model predictors, tools, software and data) that can be used by others. As mentioned earlier, the main deliverable/milestone of this work package is the implementation of a physics-based GMPE. This ultimate goal was not fully accomplished, nevertheless we present simplified GMPE as prove of concept that complementing empirical datasets with physics-based earthquake is feasible, as the variation of the synthetic data with the main shaking predictors is well understood. Due to the source complexity effects on ground motion clearly revealed by the rich synthetic data, the parameterisation adopted by the majority of empirical GMPE developers worldwide does not suffice to adequately represent the near-source characteristics of the simulated ground motions. Therefore we provided possible alternative parameterisations in which source effect from hanging wall amplification, directivity and oversaturation observed in the synthetic data are imcorporated in the functional form. This work is still an ongoing effort between ETH and swissnuclear. A final physics-based GMPE is planned to be completed by the end of 2015. Therefore the work proceeds supported by the institute of the individual researchers working on it. The tools, software and data developed during the project are not fully self sustainable because they are linked directly to an individual who in most of the cases they are not permanently in one institution, therefore the conection to each individual for data request can be easily lost when the individual move to another institute or move the direction of work.

References

Baumann C, Dalguer LA (2014) “Evaluating the Compatibility of Dynamic Rupture-Based Synthetic Ground Motion with Empirical Ground-Motion Prediction Equations”, Bulletin of the Seismological Society of America, doi:10.1785/0120130077

Cauzzi C, Faccioli E (2008) Broadband (0.05 to 20 s) prediction of displacement response spectra based on worldwide digital records. J Seismol 12:453–475. doi: 10.1007/s10950-008-9098-y

Cauzzi C, Faccioli E, Vanini M, Bianchini A (2014a) Updated predictive equations for broadband (0.01–10 s) horizontal response spectra and peak ground motions, based on a global dataset of digital acceleration records. Bull Earthq Eng. doi: 10.1007/s10518-014-9685-y.

Cauzzi C, Dalguer L, Baumann C, Giardini D (2014b) Lessons learnt by parameterising a near-field waveform dataset generated by dynamic rupture simulations. 2ECEES Istanbul.

Dalguer L, Baumann C, Cauzzi C (2013) A synthetic GMPE based on deterministic simulated ground motion data obtained from dynamic rupture models. AGU Fall Meeting 2013, San Francisco, California, USA.

Dalguer L, Cauzzi C, Baumann C, Giardini D (2014) Identification of Near-Field Ground-Motion Characteristics and Predictors Based on Synthetic Data Obtained from Dynamic Rupture Models. SSA 2014, Anchorage, AK, USA.

Douglas J, Akkar S, Ameri G, Bard P-Y, Bindi D, Bommer JJ, … Traversa P (2013) “Comparisons among the five ground-motion models developed using RESORCE for the prediction of response spectral accelerations due to earthquakes in Europe and the Middle East” Bulletin of Earthquake Engineering, 12(1), 341–358

Graizer V, Kalkan E, Lin K-W (2013) “Global Ground Motion Prediction Equation for Shallow Crustal Regions”, Earthquake Spectra, 29(3), 777–791

Gregor N, Abrahamson NA, Atkinson GM, Boore DM, Bozorgnia Y, Campbell KW, … Youngs R (2014) “Comparison of NGA-West2 GMPEs”, Earthquake Spectra, doi:10.1193/070113EQS186M

Spudich P, Rowshandel B, Shahi S, et al. (2014) Comparison of NGA-West2 Directivity Models. Earthq Spectra 140609063716004. doi: 10.1193/080313EQS222M

5. Publication Lists

5.1 Peer-Reviewed Journals

AMRA

E. Lucca, G. Festa, A. Emolo (2012). Kinematic inversion of strong motion data using a Gaussian parameterization for the slip: application to the 2008 Iwate-Miyagi, Japan, earthquake, Bull. Seism. Soc. Am., 102(6), 2685-2703.

N. Maercklin, G. Festa, S. Colombelli, A. Zollo (2012). Twin ruptures grew up to a giant earthquake. Scientific Reports , 2, 709, doi:10.1038/srep00709.

G. Festa, A. Zollo (2012). From data to source parameters: Kinematic modeling. In The Mechanics of Faulting: From Laboratory to Real Earthquakes, ISBN: 978-81-308-0502-3 Editors: Andrea Bizzarri and Harsha S. Bhat.

V. Convertito, M.Caccavale, R. De Matteis, A. Emolo, D. Wald, A. Zollo (2012). Fault extent estimation for near-real-time ground-shaking map computation purposes, Bull. Seism. Soc. Am., 102(2), 578-586, doi:10.1785/0120100306.

ETH

Baumann C. and L.A. Dalguer (2014), Evaluating the Compatibility of Dynamic-Rupture-Based Synthetic Ground Motion with Empirical GMPE. *Bull. Seismol. Soc. Am.* 104(2), April 2014, doi: 10.1785/0120130077.

S. Song, L.A. Dalguer, and P.M. Mai (2014). Pseudo-dynamic source modeling with 1-point and 2-point statistics of earthquake source parameters, *Geophys. J. Int.*, 196, 1,770-1,786.

S. Song, and L.A. Dalguer (2013). Importance of 1-point statistics in earthquake source modeling for ground motion simulation, *Geophys. J. Int.*, 192, 1,255-1,270.

INGV

Cirella, A., A. Piatanesi, M. Cocco, E. Tinti, L. Scognamiglio, A. Michelini, A. Lomax, and E. Boschi, (2009), Rupture history of the 2009 L'Aquila earthquake from non-linear joint inversion of strong motion and GPS data, *Geophys. Res. Lett*., 36, L19304, doi:10.1029/2009GL039795

Cirella A., Piatanesi A., Tinti E. Chini M. and M. Cocco (2012), "Complexity of the rupture process during the 2009 L'Aquila, Italy, earthquake", *Geophysical Journal International*.**190**, 607-621, doi:10.1111/j.1365-246X.2012.05505.x.

Scognamiglio, L., E. Tinti, A. Michelini, D. Dreger, A. Cirella, M. Cocco, S. Mazza, and A. Piatanesi (2010). Fast Determination of Moment Tensors and Rupture History: What Has Been Learned from the 6 April 2009 L'Aquila Earthquake Sequence, *Seismological Research Letters* 81, 6.

Spudich P. and A. Cirella., "Aleatory and Epistemic Uncertainties in Interpolated Ground Motions-Example from the Kasiwasaki-Kariwa Nuclear Power Plant recordings of the July 16, 2007 Niigata-ken Chuetsu-oki, Japan, Earthquake", , submitted to *Bulletin of the Seismological Society of America.*

ISTerre

Causse M., L.A. Dalguer, P.M Mai (2013). Variability of Dynamic Parameters Inferred from Kinematic Models of Past Earthquakes, accepted at *Geophysical Journal International*.

Cotton, F., R. Archuleta, M. Causse (2013). What is sigma of stress drop ?, *Seismological Research Letters* 84, 42-48.

Rodriguez-Marek, A., F. Cotton, F., N. Abrahamson, S. Akkar, L. Al-Atik, B. Edwards, G. Montalva and H. Mousad (2013). A model for single-station standard deviation using data from various tectonic regions, *Bull. Seismol. Soc. Am*., in press

KOERI

E. Harmandar, E. Cakti, M. Erdik (2013). Modeling Coherency Using Data From Istanbul Earthquake Rapid Response System. Under review.

E. Zengin, E. Cakti (2013). Ground Motion Estimations for the 2011 Van, Eastern Turkey Earthquake Using Stochastic Finite Fault Approach, submitted to Bulletin of Earthquake Engineering.

E. Harmandar, E. Cakti, M. Erdik (2012). A Method for Spatial Estimation of Peak Ground Acceleration in Dense Arrays, Geophysical Journal International, 191 (3), 1272-1284, doi: 10.1111/j.1365-246X.2012.05671.x.

METU

A. Askan, F.N. Sisman and B. Ugurhan (2013). Stochastic Strong Ground Motion Simulations in Sparsely-Monitored Regions: A Validation and Sensitivity Study on the 13 March 1992 Erzincan (Turkey) Earthquake, Soil Dynamics and Earthquake Engineering, doi: 10.1016/j.soildyn.2013.09.014.

F. Gallovič, G. Ameri, J.Zahradník, J. Janský, V. Plicka, E. Sokos, A. Askan and M. Pakzad (2013). Fault process and broadband ground-motion simulations of the 23 October 2011 Van (Eastern Turkey) earthquake, Bull. Seism. Soc. Am., 103, No. 6, doi: 10.1785/0120130044.

B. Ugurhan, A.Askan, A. Akinci and L. Malagnin (2012). Strong Ground Motion Simulations of the 2009 L'Aquila Earthquake, Italy, Bull. Seism. Soc. Am, Vol. 102, No. 4, pp. 1429–1445.

A. Askan, F.N. Sisman and O. Pekcan, A Regional Near-Surface High Frequency Spectral Attenuation (Kappa) Model for Northwestern Turkey (2014), Soil Dynamics and Earthquake Engineering, 65, 113–125. doi: 10.1016/j.soildyn.2014.06.007.

S. KarimZadeh, A. Askan, A. Yakut, G. Ameri (2013). Assessment of synthetic ground motion records obtained from alternative simulation techniques in nonlinear time history analyses of multi-story frame buildings: A case study, under review at Bull. Seism. Soc. Am.

5.2 Conference Presentations

AMRA

G. Festa, J.-P. Vilotte (2011). Role of the fault geometry on the rupture dynamics and the radiated wavefield, American Geophysical Union, Fall Meeting 2011, San Francisco,December 5-9; invited talk.

S. Del Gaudio, E. Lucca and G. Festa (2012). Strong motion simulations using coupled numerical-empirical Green's functions: the 2009 L'Aquila-earthquake. European Geophysical Union, Vienna, April 22-27.

G. Festa, A. Scala, J.-P. Vilotte (2012). How geometry and structure control the seismic radiation : spectral element simulation of the dynamic rupture of the Mw 9.0 Tohoku earthquake, American Geophysical Union, Fall Meeting 2011, San Francisco, December 3-7.

N. Maercklin, G. Festa, S. Colombelli, A. Zollo (2012). Rupture Evolution and Slip of the 2011 Tohoku Earthquake from Back-Projection of Local Seismic Data, American Geophysical Union, Fall Meeting 2012, San Francisco,December 3-7.

A. Scala, G. Festa, J.-P. Vilotte, H. Miyake (2013). How geometry and structure control the rupture dynamics of the Mw 9.0 Tohoku earthquake. IAHS, IAPSO, IASPEI Joint Assembly, Gothenborg, July 22-26.

ETH

Cauzzi C, Dalguer L, Baumann C, Giardini D (2014b) Lessons learnt by parameterising a near-field waveform dataset generated by dynamic rupture simulations. 2ECEES Istanbul.

Dalguer L, Baumann C, Cauzzi C (2013) A synthetic GMPE based on deterministic simulated ground motion data obtained from dynamic rupture models. AGU Fall Meeting 2013, San Francisco, California, USA.

Dalguer L, Cauzzi C, Baumann C, Giardini D (2014) Identification of Near-Field Ground-Motion Characteristics and Predictors Based on Synthetic Data Obtained from Dynamic Rupture Models. SSA 2014, Anchorage, AK, USA.

Song, S., L.A. Dalguer, and P.M. Mai, Pseudo-dynamic source modeling with 1-point and 2-point statistics of earthquake source parameters, annual meeting of the Southern California Earthquake Center (SCEC), Palm Springs, California, USA, 2013.

Song, S., L.A. Dalguer, and P.M. Mai, Developing a statistical framework that governs finite earthquake source process, 8th Statistical Seismology Workshop, Beijing, China, 2013.

Song, S., L.A. Dalguer, and P.M. Mai, Developing a physics-based rupture model generator (RMG) with 1-point and 2-point statistics of source parameters, IASPEI, Gothenburg, Sweden, 2013.

Song, S., P.M. Mai, and L.A. Dalguer, Pseudo-dynamic source modeling with 1-point and 2-point statistics of earthquake source parameters, annual meeting of European Geosciences Union (EGU), Vienna, Austria, 2013.

Song, S., and L.A. Dalguer, Importance of 1-point statistics in earthquake source modeling for ground motion simulation, fall meeting of American Geophysical Union (AGU), San Francisco, California, 2012.

Song, S., and L.A. Dalguer, Propagation of 1-point and 2-point statistics from dynamic source through kinematic to ground motions, ECGS Workshop , Luxembourg, 2012.

Song, S., and L.A. Dalguer, Propagation of 1-point and 2-point statistics from dynamic source through kinematic to ground motions, 15WCEE, Special Session on "Physics-based Ground Motion Simulations", Lisbon, Portugal, 2012.

Song, S., and L.A. Dalguer, Importance of 1-point statistics in earthquake source modeling for ground motion simulation, annual meeting of the Southern California Earthquake Center (SCEC), Palm Springs, California, USA, 2012.

INGV

Cirella A., Spagnolo E., Piatanesi,A., “Source Complexity: from the inversion of the kinematic rupture process to the ground motion spatial variability analysis”, S23A-2450, 2013 AGU Fall Meeting, San Francisco, 9-13 December.

Spagnuolo E., Cirella A., Piatanesi A., “Intra-event ground motion variability: Source Process of the 6th April 2009 L’Aquila, central Italy, Earthquake”, Geophysical Research Abstracts Vol. 15, EGU2013-7478, 2013 EGU General Assembly 2013, poster presentation.

Cirella A. and Spudich P. “Aleatory and epistemic uncertainties in interpolated ground motions − Example from the Kashiwazaki-Kariwa Nuclear Power Plant recordings of the July 16, 2007, Niigata-ken Chuetsu-oki, Japan, earthquake”, Geophysical Research Abstracts Vol. 15, EGU2013-5932, 2013 EGU General Assembly 2013, oral presentation.

ISTerre

Causse, M., L.A. Dalguer, P.M Mai (2012). Fracture energy scaling in dynamic models of past earthquakes as a constraints for physics-based ground-motion simulation. *Proceedings of the 15th World Conference on Earthquake Engineering*, Lisbon, Portugal.

Imtiaz, A, M. Causse, F. Cotton (2012). On the magnitude and distance dependency of the ground-motion variability: comparison between simulations and real numerical simulations and real data analysis, *Proceedings of the 15th World Conference on Earthquake Engineering*, Lisbon, Portugal.

Imtiaz, A, M. Causse, E. Chaljub, F. Cotton (2013). Magnitude and Distance Dependency of the Ground-Motion Variability from Numerical Simulations and Comparison with Real Data

Analysis, SSA 2013 annual meeting, Salt Lake City, 17-19th april, 2013. *2013 Student Presentation Award Winner*

Cornou C., N. Theodoulidis, G. Cultrera, T. Boxberger, A. Imtiaz, P.-Y. Bard, R. Bauz, S. Bayle, D. Bindi, F. Cara, R. Cogliano, C. Cretin, D. Famiani, A. Fodarella, G. Di Giulio, E. Günther, A. Konidaris, K. Makra, G. Milana, J-M. Nicole, S. Parolai, M. Pilz, S. Pucillo, G. Riccio, A. Rovelli, A. Savvaidis (2013). Ground-motion amplification and spatial variability in Argostoli basin (Cephalonia Island, Greece) inferred from a highly dense seismological network, SSA 2013 annual meeting, Salt Lake City, 17-19th april, 2013

Cornou, C. et al., 2013. Spatial variability of ground motion over short distance: insights from the small-size Argostoli basin (Cephalonia, Greece). Joint workshop JAEE-ESGWS 2013 – 10th IWSMRR, Tokyo, 24/09/2013, Invited speaker.

KOERI

E. Harmandar, E. Cakti, M. Erdik (2013). Coherency Considerations for Ground Motion Simulations, SSA Annual Meeting, Salt Lake City.

E. Zengin, E. Cakti (2013). Ground Motion Estimations for the 2011 Van, Eastern Turkey Earthquakes Using Stochastic Finite Fault Approach. SSA Annual Meeting, Salt Lake City.

METU

S. KarimZadeh, A. Askan, A. Yakut and G. Ameri (2013). Assessment of synthetic ground motion records from alternative simulation methods in dynamic response analyses of building structures. SSA Salt Lake City, USA.

G. Ameri, F. Gallovic, A.Askan and J. Zahradnik (2012). Broadband ground motion simulations of the 23 October 2011 van (eastern Turkey) earthquake. SSA San Diego, USA.

F.N. Sisman, O. Pekcan and A. Askan (2012). A regional high-frequency attenuation (kappa) model for northwestern Turkey. SSA San Diego, USA.

APPENDIX

Major scientific achievements in each institute and future directions (scientific)

AMRA

Contribution of AMRA to the Work-Package was two-pronged: we investigated the effect of the source complexity on the ground motion in the near-fault region on the one hand, and we computed broad-band strong motion synthetics on the other hand.

As for the source complexity we investigated by numerical simulations the role of the geometry on both the propagation of the rupture and the high-frequency radiation in the fault vicinity. Tackling this problem with numerical methods is difficult because the kinematic incompatibility of the slip at the geometry discontinuity results into an energy integrable singular static stress field which has to be taken into account by the numerical models. We found that a sudden change in the rupture velocity occurs when the rupture turns at the kink mainly driven by the sudden change in the dynamic normal stress. It may also occur that a change in the geometry can speed up a rupture at supershear velocities. A geometrical discontinuity behaves as a strong S wave radiator, coming from the unbalanced stress conditions on the two branches of the faults. This phase looks like a directional stopping phase, because a part of this is absorbed by the rupture that nucleates on the new branch. We observed that the amplitude of the radiation is poorly sensitive to changes in the rupture velocity while it strongly depends on the kink angle. As a consequence, the PGA shows a complex pattern, changing of one order of magnitude in the PGA when moving around the kink from directive to antidirective region.

We also included a homogeneized damage model on the fault to mimic dissipation occurring during an earthquake in the fault zone. Within this friction law, we investigated the behavior of the nucleation, the dynamic rupture and the radiation. The nucleation size is controlled by the slope of the interface law at zero slip. When assuming a large thickness of the damage layer, we also observe a stable solution according to which the traction can indefinitely increase. Because of the additional dissipation, we observed a generally slower rupture, as compared to interface frictional models and a significant reduction in the high frequency content in the near-fault records. Specifically the PGA can be reduced of one order of magnitude in the fault vicinity because of the extended damage, independently of the azimuth of the station.

As a specific case study, we investigated the role of the geometry and the structure on the radiation and rupture propagation of the Tohoku earthquake. We limited the analysis to the first stage of the earthquake and generated a large number of spectral element dynamic rupture simulations with fixed geometry and velocity model. As a general feature, we observed a different behavior of the rupture as a function of the direction of propagation: upwards the rupture goes faster and the dynamics is mostly controlled by the changes in the slope of the interface, downwards we obtained a slow rupture in its initial stage followed by a sudden acceleration at the entrance in the mantle in correspondence with a sharp change of slope. From inspection of all models, our preferred one shows a second asperity between the hypocenter and the shallow part, boosted by resonating surface waves trapped between the fault and the oceanic floor. For radiation, we can recognize that the geometrical variations are more important than structural ones. When comparing the strong motion at accelerometric network, we retrieved only the first high-frequency burst while the second wave train is likely to be associated to a complex 3-D effect of the rupture.

For the broad-band ground motion simulation, we specifically studied the L'Aquila earthquake, which showed a strong ground motion and damage variability at the scale of the fault size and for which a large amount of strong motion and aftershock data are available. For the simulations we used coupled numerical-empirical Green's functions as a propagator. High-frequencies beyond the corner frequency of the Empirical Green's functions (EGFs) were stocastically introduced into the model. To be consistent with the low frequency part of the signal, we used a kinematic source model of the earthquake. This was obtained by inversion of local strong motion data up to 0.3 Hz. This model exhibits a major slip patch between 5 and 10 km southwards of the hypocenter, which is responsible for the directivity effect observed south of the fault. We also found a smaller asperity in the upper part of the fault with slip as large as 50 cm and a third one nearby the surface, lower slip value (30 cm), which is responsible of the up-dip directivity. Rupture times indicate a faster rupture in the upper part of the fault, in the initial stage of the rupture. We then coupled this model with high frequency k^{-2} slip distributions obtained with a stochastic technique. Retrieved models were tested up to high frequencies (5-10 Hz) to provide the ground motion amplitude and its variability.

Empirical Green's functions were extracted from a dataset of more than 400 aftershocks and foreshocks with a magnitude ranging between 2.5 and 4.8 based on location, stress drop, magnitude and signal to noise ratio. At low frequencies 1D numerical Green's functions were computed via a discrete wavenumber- finite-element method while 3D Green's functions were estimated by the spectral element method. Broadband signals are obtained by coupling the low frequency part with high frequency simulations computed using EGFs and compared with real data both for near source and far source stations. We found that near fault stations reveal complex waveforms, that require an accurate modelling of the source/propagation coupling. For the L'Aquila case, the source model needs to be coupled with a 3D modelling of the basin to retrieve the right frequency content in the low/intermediate range (0.5-1Hz). A primary role in the strong motion generation is played by the variability of the rise time on the fault. The synthetic spectrum at high frequency well fit the real one when the rise time rapidly changes in a broad interval (0.1s to 1s). Changes in the slip roughness play a secondary role. Selection of EGF is a critical point for correct modelling of the ground motion.

Changing the EGF can lead to changes in the Fourier and response spectra of one order of magnitude in near fault at some frequencies. Far field data are well constrained by the average model. Fourier spectrum sigma is less than one order of magnitude. In near fault, some frequencies appear underestimated and the sigma in the Fourier spectrum is larger than one order of magnitude. These latter simulations were realized in collaboration with ISTerre group, that provided a code for accounting for source variability

ETH

Quantifying the variability of finite earthquake source process and investigating its relationship to near-source ground motion characteristics

One of the main research objectives at ETH is to develop a statistical framework in which we can quantify the variability of finite earthquake source process and investigate the characteristics and variability of near-source ground motions. We first quantify the variability of input parameters in spontaneous dynamic rupture modelling in the framework of 1-point and 2-point statistics and analyse resulting kinematic source and ground motions. This study clearly shows that the variability of earthquake source and ground motions can be efficiently quantified in the framework of 1-point and 2-point statistics and in particular 1-point statistics of input source parameters needs to be more explicitly considered in future source-modelling studies. We also develop a pseudo-dynamic rupture model generator (SongRMG) with 1-point and 2-point statistics of kinematic source parameters and test its efficiency with a set of dynamically derived rupture models. We demonstrate that the newly developed rupture model generator (stochastic modelling) can successfully reproduce the core features of dynamic rupture models and it can be used to investigate the sensitivity of near-source ground motion characteristics to source (correlation) statistics in a systematic way.

We plan to improve and strengthen the stochastic finite source modelling method we developed in this project in various ways: 1) We will investigate the effect of fracture energy on kinematic source correlation statistics, 2) We will develop a more generalized version of PD models, 3) we also try to extend the PD modelling method to high frequencies (> 1Hz).

Another main activity of ETH was the development of ground-motion prediction equations (GMPEs) based on synthetic data obtained from physics-based dynamic rupture simulations. Selectively presented in this contribution are the key results obtained by parameterising the near-field synthetic waveforms (Baumann and Dalguer, 2014) in the moment magnitude range $5 < M_W < 7+$ relevant for seismic hazard studies in central and western Europe. Developing predictive equations using synthetics allows: a) to overcome the difficulties posed by the paucity of near-field data in the calibration datasets of empirical GMPEs; b) to expand our understanding of source-dominated ground-motion phenomena; c) to investigate the characteristics of “noise-free” long-period ground motions. We identify the main explanatory variables by analysing the variation of the synthetic peak ground-motions and response spectral ordinates as a function of different predictors, including earthquake source parameters in addition to classical source-to-site path terms. Our approach is largely based on verifying whether the common predictive equations used in empirical and semi-empirical GMPEs (Gregor et al., 2014; Douglas et al., 2014) are appropriate for the parameterisation of our synthetic data suite. Corrective terms or alternative functional forms are introduced if supported by the synthetic data. Emphasis is placed on the impact of using different finite-fault distance metrics on the predictions, with special reference to the oversaturation (Baumann and Dalguer, 2014; Graizer et al., 2013) of peak-motion amplitudes apparent from our synthetics at distances smaller than the depth to the top of rupture. .

INGV

‘**Source Complexity: from the inversion of the kinematic rupture process to the ground motion spatial variability analysis**’

Cirella A., Piatanesi A., Spagnuolo E.

The summarized work is carried out in the framework of Task 1 (Modeling of source complexity: kinematic and dynamic rupture models) and Task 2 (Identification of strong ground motion dominated by source effects at low frequency) of JRA3. Our main goals were:
I. to retrieve a complete kinematic description of the rupture process of the 2009 M_w 6.1 L’Aquila earthquake;
II. to study the *spatial variability* of the ground motion induced by the source of the 2009 M_w 6.1 L’Aquila earthquake, by computing shaking scenarios;
III. to quantify the *scatter* of ground motion parameters, predicted at several recording stations;

In order to achieve the first goal, we investigated the rupture history of the 2009 April 6th (M_w6.1) L’Aquila normal faulting earthquake by using a non-linear inversion of strong motion, GPS and DInSAR data. Both the separate and joint inversion solutions reveal a complex rupture process and a heterogeneous slip distribution. Slip is concentrated in two main asperities: a smaller shallow patch of slip located up-dip from the hypocentre and a second deeper and larger asperity located south-east wards along-strike direction. The key feature of the source process emerging from our inverted models concerns the rupture history, which is characterized by two distinct stages. The first stage begins with rupture nucleation and with up-dip propagation at relatively high (~4.0km/s), but still sub-shear, rupture velocity. The second stage starts nearly 2.0–2.5s after nucleation and it is characterized by the along-strike rupture propagation. The largest and deeper asperity fails during this stage of the rupture process. The rupture velocity is larger in the up-dip than in the along-strike direction. The up-dip and along-strike rupture propagation are separated in time and associated with a Mode II and a Mode III crack, respectively. Our results show that the L’Aquila earthquake featured a very complex rupture, with strong spatial and temporal heterogeneities suggesting a strong frictional and/or structural control of the rupture process.

Our second aim was focused on the identification of the spatial variability of the ground motion parameters in relation to the heterogeneities of the source. To accomplish this goal, we analyzed the intra-event ground motion variability associated to the source process of the L’Aquila earthquake. We know that the accurate evaluation of a ground motion intensity measure for future earthquakes is necessary to inform earthquake-engineering decision. One widely adopted strategy is the probabilistic approach that uses the ground motion predictive equations to assess a ground motion intensity measure. Nevertheless at present the available empirical models are not able to comprehensively predict the high spatial heterogeneity of the observed ground motion. One key issue is related to the fact that the contribution of each explanatory variable to the ground motion variability is still unclear. In this framework we investigated the ground motion variability through a posteriori analysis of a well instrumented past earthquake, the 2009 L'Aquila (central Italy) M_w 6.1 earthquake. As explained before, the joint inversion of strong motion, GPS and DInSAR data allowed us to image the coseismic rupture history on the fault plane. The retrieved source model not only features the slip distribution, but also provides an entire ensemble of models (N=2000) generated during the search stage of the inversion and a rupture velocity field, which reflects the mechanical properties of the fault. This information is valuable in order to investigate the ground motion variability. In order to quantify the source parameters contribution to the ground motion variability we fixed the rupture velocity field and the seismic moment ($M_0 = 3.5\times10^{18}$Nm) to model scenarios for a single fault plane (the same of the 2009 L’Aquila earthquake) on a ‘virtual’ grid (800 sites) of observers around the fault. We varied the slip distribution and the nucleation position by considering a heterogeneous rupture time distribution for each nucleation point. The amount of models guarantees the statistical consistency of the dataset. From those sets of scenarios we extracted several ground motion parameters: PGD, PGV, SA at different oscillator periods. The huge quantity of synthetic data is then treated statistically to recognize local features of the ground motion (e.g. directivity) and to try to answer key questions (such as: was the L'Aquila earthquake expected? Was it the worst-case scenario?) The obtained results show how the nucleation position on the fault plane is relevant for the ground motion analysis also at low-intermediate frequency; moreover, it seems that the L'Aquila earthquake may not be intended as the *worst-case* scenario. In this framework we want to extend the sensitivity analysis to other kinematic parameters describing the source process, in order to investigate how the variation of the source parameters affect the variability of ground motion prediction. In particular we are focusing our attention to accounts for slip distributions, i.e. the relative position of the patch of slip respect to the hypocenter location, which could strongly influence the ground motion variability. For this part of the work we are collaborating with Elena Spagnuolo (INGV researcher).

The third objective was on the use of earthquake source inverted rupture model as a possible source of aleatory and epistemic uncertainties in interpolated ground motion analysis. This idea was born from the collaboration with Paul Spudich (researcher USGS), during which we chose to study the 2007 Niigata-ken Chuetsu-oki earthquake, because it is one of the few large events whose causative fault extends beneath a nuclear power plant, the Kashiwazaki-Kariwa nuclear power plant (KKNPP), where a peak ground acceleration associated with surface motions exceeding 1200 gals has been recorded. We quantified the scatter of absolute spectral acceleration, SA, predicted at KKNPP from rupture models derived from waveform inversion of a set of Niigata-area accelerograms. This approach has allowed us to study the variability of predicted motion at KKNPP from the non-uniqueness of the rupture inversion. Inspired by this work we'd like to extend it on the L'Aquila earthquake analysis.

ISTerre

The contribution of ISTerre has been reported in deliverables D13.1, D13.2 and D13.4. What we list here are basically future directions that are needed to complements the efforts of the work package.

- friction laboratory experiments will help getting insights on the source parameters statistics (stress drop, rupture velocity) and earthquake energy balance (strain energy, fracture energy, radiated energy).

- to perform additional numerical simulations of ground motion in the near-source by using a larger set of "realistic" kinematic models, all extracted from the database of finite-source rupture models. This will allow to derive robust insights on both the within-event and the between event components of the variability in the near-field.

- to compare the site-specific spatial variability measured in Argostoli basin with the one observed at other dense arrays (e.g. SMART1, Chiba), especially by comparing the standard deviation of the residuals as a function of interstation spacing. This will greatly constrain spatial correlation models at local-to-regional that are used in shake-maps and lifeline PSHA studies.

KOERI

The project has promoted the study of the 1999 Kocaeli earthquake in terms of both high frequency and long period simulation of the wave propagation, leading to better understanding the effects of the 3D velocity structure of the region. This understanding and the results of the simulations are very helpful for the estimation of the wave propagation from future events that are expected to occur on the western continuation of the North Anatolian fault in the Marmara Sea.

The project has also promoted the study of a more recent earthquake that occurred in Eastern Turkey, namely the 2011 M7.1 Van earthquake. This event took place on a previously unrecognized fault and was sparsely recorded. Stochastic simulation of the strong ground motion has been carried out for the main- and one major after-shock of this event. This work has been carried out as part of a PhD study.

Understanding the spatial variability of earthquake ground motion can be important for the response of linear lifelines such as bridges, pipelines, communication systems, and should preferably be accounted for in their design. In addition to global models, region specific models representing spatial variability and coherency characteristics need to be developed. For Istanbul we have developed a coherency model that can be used for the assessment and simulation of spatially variable ground motion in Istanbul. A procedure was developed to generate earthquake ground motions that are compatible with given target response spectrum and that have coherencies consistent with the coherency model generated for Istanbul. The approach can ultimately be used as the skeleton towards an automated system to simulate the ground motion consistent with the coherency characteristics of a region at stations distributed linearly or over an extended area. Furthermore it potentially can be implemented to Shake Map type applications.

METU

Within the course of this project, METU team has performed a wide set of scientific studies ranging from source inversions to broadband simulations; from site characterizations to direct engineering applications of synthetic ground motion datasets. We had the chance to interact with other institutes at meetings as well as electronic communications whenever necessary. The outcomes of this project are believed to be successful examples of interdisciplinary research.

The major scientific achievements of METU within the course of NERA project are as follows:

- On October 23, 2011, Mw 7.1 earthquake occurred in Eastern Turkey, close to Van and Erciş towns, causing more than 600 casualties and a widespread structural damage. The earthquake ruptured a 60-70 km long NE-SW fault with a thrust mechanism, in agreement with regional tectonic stress regime. Within this work package, METU team along with other researchers (please see the related publication) studied the fault process of the event and the recorded ground motions using different sets of data. This fault was not a previously known/studies fault, nor was it mapped on the active fault map of Turkey. In addition, the mainshock of the event was recorded only by 3 strong motion stations within an epicentral distance of 100 km. Under the given conditions, it was invaluable to be able to predict the “not recorded” ground motions though careful studies of the source and wave propagation characteristics in the region. Thus, METU team had the chance to work with earth scientists from other institutes to study both the source process as well perform ground motion simulations in a region with very sparse data. We showed that the only models comprising source complexities, such as a delayed rupture of shallow asperities, enable explanation of the acceleration record at the only available near-fault station, which exhibits a long duration and two prominent wave groups. These complex rupture models are used to simulate the ground motion in the near-fault area, specifically, at Van and Erciş, where records of the mainshock were missing, providing reasonable agreement with the observed spatial distribution of damage. Related publications are presented below.

- On 6 April 2009, an earthquake of Mw 6.1 occurred in central Italy, close to the town of L’Aquila. Although the earthquake is considered to be a moderate-size event, it caused extensive damage to the surrounding area. The event is identified with significant directivity effects: high amplitude, short-duration motions are observed at the stations that are oriented along the rupture direction, whereas low-amplitude, long-duration motions are observed at the stations oriented in the direction opposite to the rupture. The complex nature of the earthquake combined with its damage potential brings the need for studies that assess the seismological characteristics of the 2009 L’Aquila mainshock. Within the course of NERA project, METU team has performed ground motion simulations with alternative methods of varying accuracy; studied carefully the model parameters that define the ground motions physically and realistically. Though alternative methods to generate the same set of observed records, we demonstrated the importance of choosing the critical region-specific source, propagation and site parameters and their influence on the simulated ground motions. We also showed that most of the observed complexity can be explained when properly combining site specific and finite-fault effects. It is also observed that purely composite and/or stochastic models without the possibility of modeling the coherent low-frequency wavefield by the integral approach would meet difficulties when explaining the near-source directivity pulses observed at near-field stations. Correct modeling of pulse-type records is of great relevance to structural engineering because their seismic demand and spectral shape are different with respect to ordinary records and can generate much higher damage. Related publications are presented below.

- One approach to model the high-frequency attenuation of spectral amplitudes of S-waves is to express the observed exponential decay in terms of Kappa (□□ factor. Kappa is a significant parameter used for identifying the high-frequency attenuation behavior of ground motions as well as one of the key parameters for stochastic strong ground motion simulation method. There is not yet a systematic investigation of the Kappa parameter based on the recently-compiled Turkish ground motions. Within NERA- JRA3- WP13, we examined a strong ground motion dataset from Northwestern Turkey with varying source properties, site classes and epicentral distances. METU team has investigated the high-frequency spectral decay (kappa) parameter computed from 174 records (522 components) measured at 15 different strong motion stations from 142 earthquakes with magnitudes 3.0<Mw<6.0 in Northwestern Turkey. The effects of magnitude, site class and distance on kappa values are investigated for both the horizontal and vertical components. A regional model is also presented for future use in stochastic simulations and GMPE adjustments. Based on 5% confidence interval, t-tests indicate no linear relation of kappa on earthquake magnitude for the dataset employed. However, site class influences the computed kappa values significantly. Our numerical results for zero-distance kappa values are consistent with the worldwide data and the previous findings from smaller datasets in the same region. Related publications are presented below.

- As an effective link between engineering and earth sciences, METU team has performed analyses to provide insights into the nonlinear dynamic behavior of typical frame structures to real records of a particular event versus the corresponding synthetic records. The key question here is whether the seismologically “acceptable” synthetic ground motion records can be used for earthquake engineering purposes without any prior scaling or modification of the records. We also investigated if the misfits in terms of seismological measures (such as Fourier Amplitude Spectrum) between the real and simulated records correspond to consistent differences in engineering demand parameters. This study and similar research are particularly useful for evaluating synthetics in terms of engineering performance measures in regions with scarce strong ground motion records. We found that the match between the Fourier Amplitude Spectrum of the real and synthetic record around the frequencies that correspond to the fundamental period of the structure governs the nonlinear response. Thus, it is important to simulate realistic amplitudes over the entire broadband frequency range of interest for earthquake engineering purposes in order to cover all types of buildings with a range of fundamental periods. Related publications are presented below.

- Finally, physics-augmented-GMPEs being the main objective and milestone of this work package is considered, METU team (along with the ETH team) has proposed a fully synthetic GMPE based on the set of dynamic rupture simulations obtained from ETH. We tested the functional form carefully. The regression analyses were performed using a maximum likelihood approach and the random effects model is used to separate the within-event and between-event variabilities. In this study, we took advantage of the ground motion dataset generated by dynamic rupture simulations to test the dependence of near-fault ground motions and in particular of between-event and within-event residuals on physical parameters of the rupture process. In summary, from between-event residuals we have observed a clear dependency on rupture velocity and maximum stress drop. On the other hand, no apparent correlation is found between residuals and average stress drop. We also showed that the within-event residuals correlate with source-station positions. For future studies, we suggest studying the correlation between the mentioned source parameters and main seismological parameters (Mw, R, general crust properties) and including these effects into the functional forms that exhibit more of earthquake physics.